Estimation of Transmission Loss in the Presence of Geoacoustic Inversion Uncertainty

Peter Gerstoft, Chen-Fen Huang, *Student Member, IEEE*, and William S. Hodgkiss, *Member, IEEE*

***Abstract*—A common problem in sonar system prediction is that the ocean environment is not well known. Utilizing probabilistic based results from geoacoustic inversions we characterize parameters relevant to sonar performance. This paper describes the estimation of transmission loss and its statistical properties based on posterior parameter probabilities obtained from inversion of ocean acoustic array data. This problem is solved by first finding an ensemble of relevant environmental model parameters and the associated posterior probability using a likelihood based inversion of the acoustic array data. In a second step, each realization of these model parameters is weighted with their posterior probability to map into the transmission loss domain. This approach is illustrated using vertical-array data from a recent benchmark data set and from data acquired during the Asian Seas International Acoustics Experiment (ASIAEX) 2001 in the East China Sea. The environmental parameters are first estimated using a probabilistic-based geoacoustic inversion technique. Based on the posterior probability that each of these environmental models fits the ocean acoustic array data, each model is mapped into transmission loss. This enables us to compute a full probability distribution for the transmission loss at selected frequencies, ranges, and depths, which potentially could be used for sonar performance prediction.**

***Index Terms*—Geoacoustic inversion, SAGA, sonar performance prediction, transmission loss prediction.**

I. Introduction

A WEAKNESS in sonar performance prediction has been the lack of means for quantifying the impact of uncertainty in estimates of the ocean environment. In the last decade, there has been much work done on inversion of geoacoustic parameters and their associated uncertainty [1]–[7]. An important problem is how to translate these parameters and their associated uncertainties into other domains where information can be used. In this paper, we will develop and show a method for translating this uncertainty into a utility domain, the transmission loss (TL) domain. The TL domain is important as it can be used in connection with sonar performance prediction (e.g., [8] and in particular [9]).

Fig. 1 summarizes the prediction of TL (usage domain) from ocean acoustic data observed on a vertical or horizontal array (data domain). The geoacoustic inverse problem is solved as an intermediate step to find the posterior probability distribution (PPD) of environmental parameters $p(\mathbf{m}|\mathbf{d})$ (environmental domain). We are not directly interested in the environmental parameter estimates itself but rather better statistical prediction of the TL field, the usage domain $\mathbf{u}$. Based on the posterior distribution $p(\mathbf{m}|\mathbf{d})$, the predictive probability distribution of the transmission loss $p(\mathbf{u})$ is obtained via Monte Carlo simulation. From this TL probability distribution, all relevant statistics of the TL can be obtained, such as the median and percentiles.

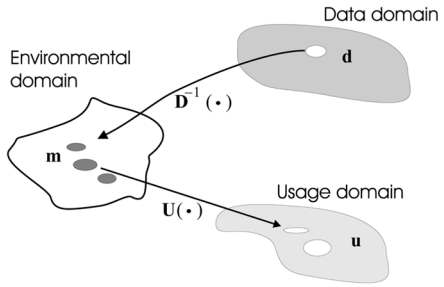

Fig. 1. Observation $\mathbf{d}$ is mapped into a distribution of environmental parameters $\mathbf{m}$ that potentially could have generated it. These environmental parameters are then mapped into the usage domain $\mathbf{u}$.

Both the experimental data $\mathbf{d}$ and the usage domain model $\mathbf{u}$ are related to $\mathbf{m}$ via forward models $\mathbf{D}(\mathbf{m})$ and $\mathbf{U}(\mathbf{m})$ corresponding to $\mathbf{d}(\mathbf{m})$ and $\mathbf{u}(\mathbf{m})$, respectively. Thus, formally we have $\mathbf{u} = \mathbf{U}(\mathbf{D}^{-1}(\mathbf{d}))$. However, this direct mapping is ill-posed and is instead interpreted probabilistically where we also can include prior information. It is assumed that the mapping $\mathbf{D}(\mathbf{m})$ and $\mathbf{U}(\mathbf{m})$ are deterministic, so that all uncertainties are in the data and environmental parameters. However, in [10] and [11], the forward mapping is assumed to be probabilistic.

A. Overview of Algorithm

The principle of the inversion is indicated in Fig. 1. Based on the ocean acoustic data $\mathbf{d}$, we statistically characterize TL (the usage domain $\mathbf{u}$). The vector $\mathbf{d}$ represents the acoustic data observed at N hydrophones and the vector $\mathbf{u}$ represents TL at several ranges and depths. As shown in Fig. 1, this is mapped via a set of M environmental parameters $\mathbf{m}$. The approach involves a number of steps as outlined here.

1) Determine an environmental parametrization for the ocean acoustic environment and select an appropriate propagation model. This defines the mapping $\mathbf{D}(\mathbf{m})$ from the environmental domain $\mathbf{m}$ to the data domain $\mathbf{d}$.
2) Determine the mapping $\mathbf{U}(\mathbf{m})$ from the environmental domain $\mathbf{m}$ to usage domain $\mathbf{u}$. Except for a change in geometry, here, this is similar to the mapping used to determine $\mathbf{D}(\mathbf{m})$, however, could be any other mapping.
3) Find acceptable model parameters $\mathbf{m}$ from the acoustic array data. As indicated in Fig. 1, a region around the data can map into several acceptable solutions in the environmental model domain.

Manuscript received April 22, 2004; revised June 1, 2005; accepted June 13, 2005. This work was supported by the Office of Naval Research under Grants N00014-01-0171 and N00014-05-1-0264. **Guest Editor: P. Abbot.**

The authors are with the Marine Physical Laboratory, University of California San Diego, La Jolla, CA 92093-0238 USA (e-mail: gerstoft@ucsd.edu).

Digital Object Identifier 10.1109/JOE.2006.875104

4) Map the acceptable models $\mathbf{m}$ into the usage domain $\mathbf{u}$. Several environmental models can map into the same usage region.

As indicated in Fig. 1, the mapping from data to usage domain is nonunique. There are many environmental models that give about the same goodness-of-fit. The maximum-likelihood (ML) estimate of the environmental model gives the most likely fit. Instead of using just one estimated environment, it is proposed to describe the environmental solution probabilistically. This probability is then mapped into the usage domain. Knowing the PPD in the usage domain is preferable to having a single point estimate such as the usage domain result corresponding to the ML solution.

II. Inverse Problem Framework

In the Bayesian paradigm, the solution to determining parameters of interest $\mathbf{m}$ given an observation $\mathbf{d}$ is characterized by the posterior probability $p(\mathbf{m}|\mathbf{d})$. First, the prior information about the model parameter vector is quantified by the probability density function $p(\mathbf{m})$. Then, this information is combined with the likelihood function $p(\mathbf{d}|\mathbf{m})$ provided by the combination of data and the physical model to give the posterior information of the model parameters $p(\mathbf{m}|\mathbf{d})$. A clear discussion of inverse theory from a probabilistic point of view is given by Tarantola [12]. Additional details of Monte Carlo sampling of posterior probabilities can be found in [2], [6], [10], [13], and [14]. The solution to the inverse problem is then

$$\begin{aligned} p(\mathbf{m}|\mathbf{d}) &= \frac{p(\mathbf{d}|\mathbf{m})p(\mathbf{m})}{p(\mathbf{d})} \\ &\propto \mathcal{L}(\mathbf{m})p(\mathbf{m}) \end{aligned} \tag{1}$$

where $p(\mathbf{d})$ is a normalizing factor that makes the posterior probability density $p(\mathbf{m}|\mathbf{d})$ integrate to one; since it does not depend on environmental model $\mathbf{m}$, it is typically ignored in parameter estimation. In the second representation, the normalization constant $p(\mathbf{d})$ is omitted and a brief notation $\mathcal{L}(\mathbf{m})$ is used to denote the likelihood function $p(\mathbf{d}|\mathbf{m})$. The posterior distribution $p(\mathbf{m}|\mathbf{d})$ carries all information available on models originating from the data and from data-independent prior information. From this distribution all relevant features of the environment can be found such as the maximum *a posteriori* (MAP) estimator.

The PPD $p(\mathbf{m}|\mathbf{d})$ is M-dimensional, where M is the dimension of $\mathbf{m}$. How to compute the posterior distribution $p(\mathbf{m}|\mathbf{d})$ depends on the dimension M. For small problems, $M \leq 5$, evaluating the likelihood function over a grid of parameter values seems most efficient. For medium scale problems, Monte Carlo Metropolis sampling [6], [15] is most efficient. For large scale problems, sampling the PPD is impractical and it is necessary to compute the posterior distribution using Gaussian assumptions which do not require extensive sampling of the posterior distribution, e.g., see [16].

In order to develop the present method, we focus on small scale problems and thus the posterior distribution $p(\mathbf{m}|\mathbf{d})$ is evaluated by sampling the distribution over a grid of parameter values.

A. Probability of $\mathbf{u}$

We are not only interested in the environment itself but also better estimates in the information usage domain $\mathbf{u}$. Based on the posterior distribution $p(\mathbf{m}|\mathbf{d})$, the distribution $p(\mathbf{u})$ is obtained and from this distribution all relevant statistics of the usage domain can be obtained. In the present application, the usage domain is transmission loss.

For either the posterior or prior probability distribution of the environmental parameters, the probability distribution of $\mathbf{u}$ is obtained

$$p(\mathbf{u}) = \int_{\mathcal{M}} \delta[\mathbf{U}(\mathbf{m}) - \mathbf{u}]p(\mathbf{m})\, d\mathbf{m} \tag{2}$$

where $\mathcal{M}$ represents the environmental model domain. This integral is implemented numerically by using samples from the model domain $\mathbf{m}$ based on the probability distribution $p(\mathbf{m})$ and then binning $\mathbf{U}(\mathbf{m})$. For the posterior, it is implemented by first doing an inversion to determine $p(\mathbf{m}|\mathbf{d})$ and storing the environmental samples $\mathbf{m}_i$ found in the inversion. These samples are then reused to compute the TL.

As the full probability distributions are available and are not necessarily Gaussian, it is preferable to characterize the distributions with medians and percentiles instead of means and standard deviations. Since the distributions are not symmetric around the medians, neither are the percentiles.

B. Likelihood and Objective Function

This section derives a likelihood function to be used in the probabilistic inversion following the same approach as described in [2] and [17]. The relation between the observed complex-valued data vector $\mathbf{d}(\omega_l)$ on an N-element hydrophone antenna array and the predicted data $\mathbf{D}(\mathbf{m}, \omega_l)$ at an angular frequency ω_l is described by the model

$$\mathbf{d}(\omega_l) = \mathbf{D}(\mathbf{m}, \omega_l) + \mathbf{e}(\omega_l) \tag{3}$$

where $\mathbf{e}(\omega_l)$ is the error term. The predicted data is given by $\mathbf{D}(\mathbf{m}, \omega_l) = \mathbf{d}(\mathbf{m}, \omega_l)s(\omega_l)$, where the complex deterministic source term $s(\omega_l)$ is unknown. The transfer function $\mathbf{d}(\mathbf{m}, \omega_l)$ is obtained using an acoustic propagation model and an environmental model $\mathbf{m}$ [18]. For simplicity, data from only one frequency is assumed. However, the theory for multifrequency is also described in [2] and [17].

Assume the errors $\mathbf{e}$ to be Gaussian distributed with zero mean and covariance $\mathbf{C}_d$. The errors represent all features that are not modeled in the data such as noise, theoretical errors, and modeling errors. Hence, the likelihood function is

$$\begin{aligned} \mathcal{L}(\mathbf{m}, \mathbf{C}_d, s) &= \pi^{-N}|\mathbf{C}_d|^{-1} \\ &\quad \times \exp\left(-[\mathbf{d} - s\mathbf{d}(\mathbf{m})]^\dagger \mathbf{C}_d{}^{-1}[\mathbf{d} - s\mathbf{d}(\mathbf{m})]\right) \end{aligned} \tag{4}$$

where N is the number of data points and superscript $\dagger$ denotes the complex conjugate transpose. Although strictly speaking it is not true, for convenience we assume $\mathbf{C}_d = \nu\mathbf{I}$. The source term s can be estimated in closed form by requiring $(\partial \log \mathcal{L}/\partial s) = 0$, whereby

$$s_{\mathrm{ML}} = \frac{\mathbf{d}^\dagger \mathbf{d}(\mathbf{m})}{||\mathbf{d}(\mathbf{m})||^2}. \tag{5}$$

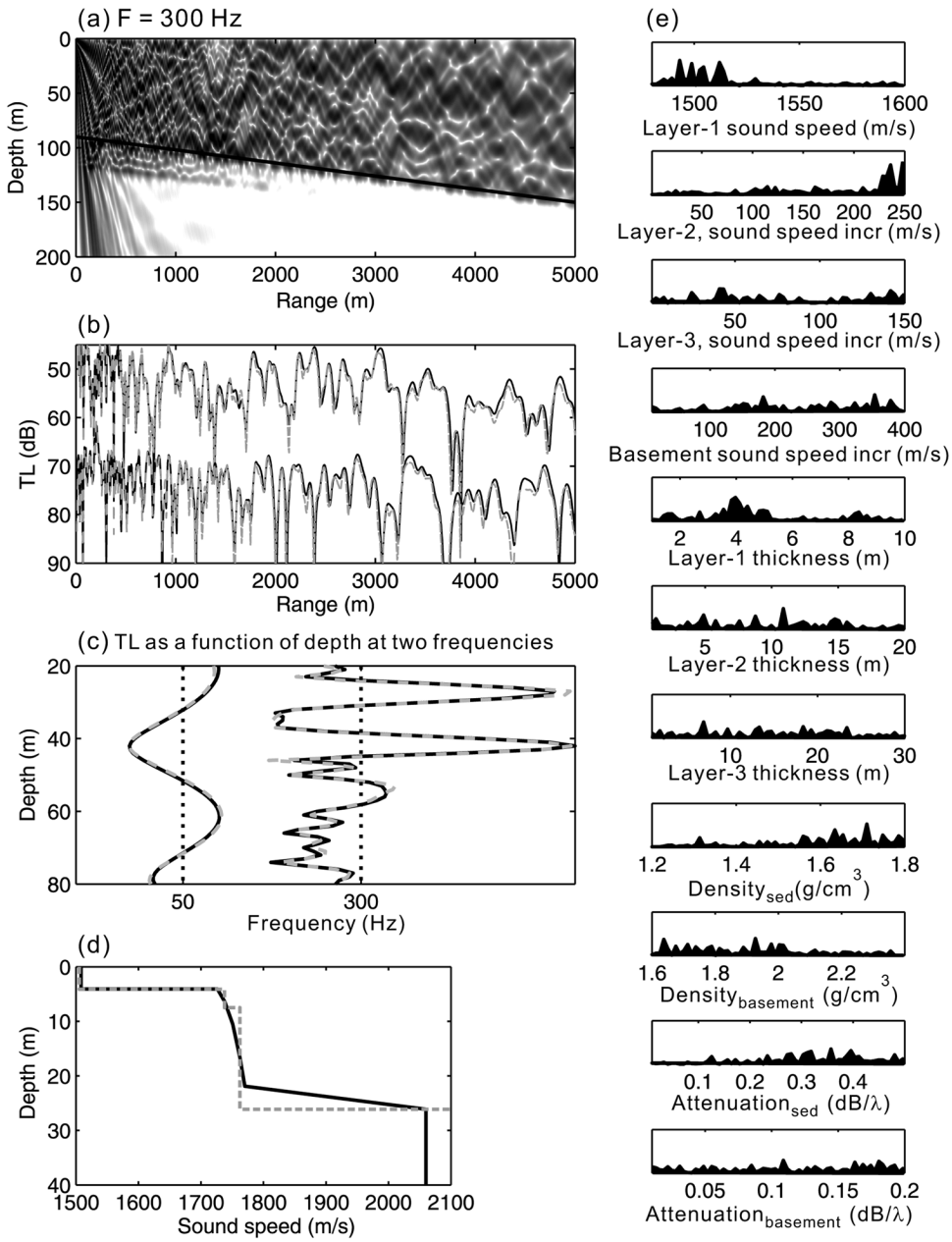

Fig. 2. Inversion results for TC1 using vertical array data at 0.5 km (see the text for the details).

It is seen that s depends on $\mathbf{m}$ but not on ν. After substituting s_{ML} back into (4), the likelihood function is then

$$\mathcal{L}(\mathbf{m},\nu) = \frac{1}{\pi^N \nu^N} \exp\left(-\frac{\phi(\mathbf{m})}{\nu}\right) \tag{6}$$

where

$$\phi(\mathbf{m}) = \|\mathbf{d}\|^2 - \frac{|\mathbf{d}^\dagger \mathbf{d}(\mathbf{m})|^2}{\|\mathbf{d}(\mathbf{m})\|^2} \tag{7}$$

is the objective function. The ML estimate of the noise ν_{ML} can be estimated in closed form by solving $(\partial \log \mathcal{L}/\partial \nu) = 0$

$$\nu_{\mathrm{ML}} = \frac{\phi(\mathbf{m})}{N}\,. \tag{8}$$

The ML solution of the model parameter vector $\mathbf{m}_{\mathrm{ML}}$ is obtained by maximizing the objective function over all $\mathbf{m}$. Finally, an overall estimate for the error power ν is obtained from (8) at the environmental ML solution: $\nu_{\mathrm{ML}}(\mathbf{m}_{\mathrm{ML}})$ and can be reinserted into the likelihood function. For simplicity, we consider the error as known and only keep the free argument $\mathbf{m}$ of the objective function ϕ. This approach leads to [2]

$$\mathcal{L}(\mathbf{m}) = \left[\frac{N}{\pi \phi(\mathbf{m}_{\mathrm{ML}})}\right]^N \exp\left[-N\frac{\phi(\mathbf{m})}{\phi(\mathbf{m}_{\mathrm{ML}})}\right]. \tag{9}$$

The previous derivation assumes that the error in each sample is not correlated with the next sample. In practice these samples are correlated. One argument is that there cannot be more independent information than the number of propagating modes [2]. The number of samples N in the previous equations must be replaced with the effective number of samples N_{eff}.

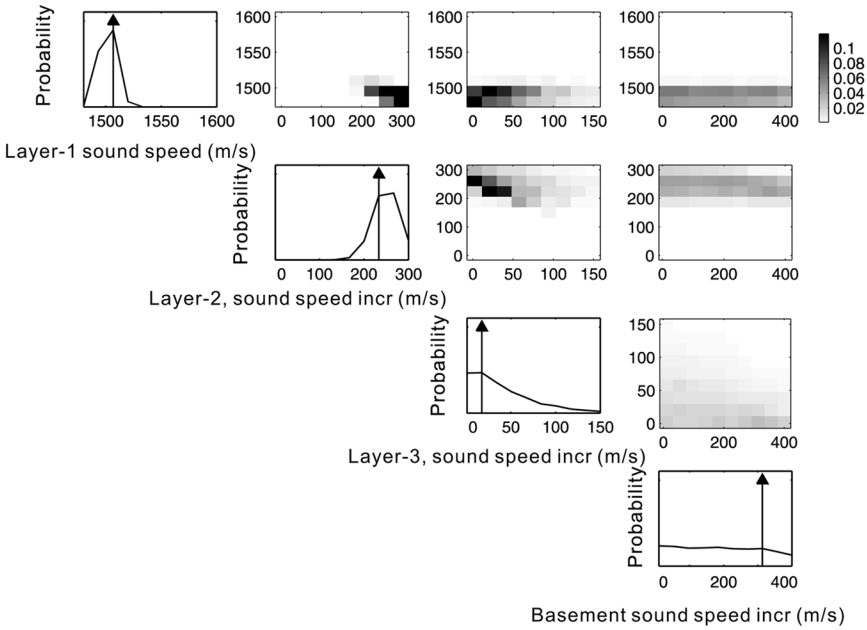

Fig. 3. 1-D and 2-D marginal probability distributions for bottom sound-speed profile for TC1. The vertical arrow indicates the ML solution (SAGA best fit). Note that the maximum in the marginal distribution might not correspond to the ML estimate.

III. Examples

Two examples are used to illustrate the approach. The first example (described in Sections III-A and B) is based on Test Case 1 (TC1) of the geoacoustic inversion workshop [19] sponsored jointly by the Office of Naval Research (ONR) and the Space and Naval Warfare Systems Command (SPAWAR). The second example (Sections III-C and D) is based on real data taken from the ASIAEX 2001 East China Sea experiment [20]. For both examples, we first carry out an inversion to obtain the posterior probability $p(\mathbf{m}|\mathbf{d})$ as discussed in Section II-B and then estimate the probability of the TL using (2).

As described in Sections III-A and C, we first do a full inversion and then an exhaustive inversion for a few of the more important parameters. The reason for the two-step inversion procedure is to be sure that the posterior probabilities $p(\mathbf{m}|\mathbf{d})$ is sampled sufficiently dense so the transmission loss probability is correct. Ideally, these two inversions could be combined into one step.

Both examples were solved using the standard inversion package SAGA [1], [21]. SAGA is a software package that helps the user determines the best set of parameters to match a given data set. SAGA has integrated some of the best ocean acoustic and electromagnetic forward model codes into the inversion and can handle many types of data. As its main thrust, it uses genetic algorithms (GA), but also exhaustive search, simulated annealing, very fast simulated annealing, Cramer–Rao bounds, and Monte Carlo Metropolis sampling is used.

A. TC1—Inversion

In the recent geoacoustic inversion workshop, several range dependent bottoms with a complicated geoacoustic structure were supplied. Here we focus on TC1. TC1 represents a monotonic downslope propagation with the bathymetry ranging from 90 m (0-km range) to 150 m (5-km range). The ocean sound-speed profile is downward refracting and is given by $c_w(z) = 1495 - 0.4z$, where z is the water depth in meters. The source depth is 20 m. The data were generated by the fidelity parabolic equation RAMGEO code [22]. There was no uncertainty in recording geometry and both amplitude and phase were provided. For the present application, we use the vertical array data at 0.5-km range at frequencies 50 and 300 Hz to do the inversion. The bottom is modeled as a three-layered sediment overlying a basement where the thickness and the sound speeds of each layer are the unknown model parameters. It should be pointed

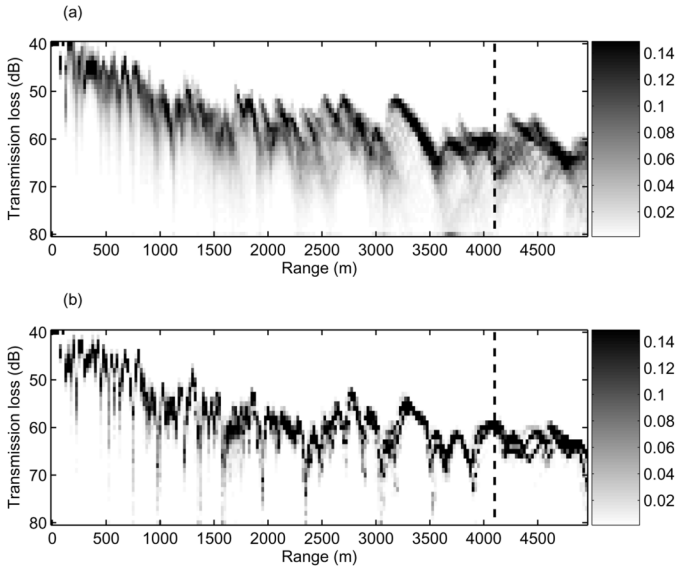

Fig. 4. (a) Prior and (b) posterior probability distributions for TL versus range at 80-m depth for TC1.

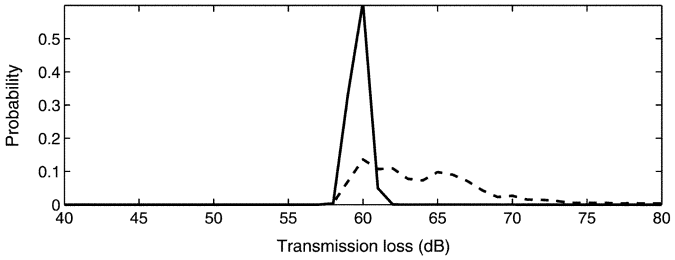

Fig. 5. Posterior (solid) and prior (dashed) probabilities of TL at 4200-m range and 80-m depth. These correspond to a cut (vertical dashed lines) though the contours in Fig. 4.

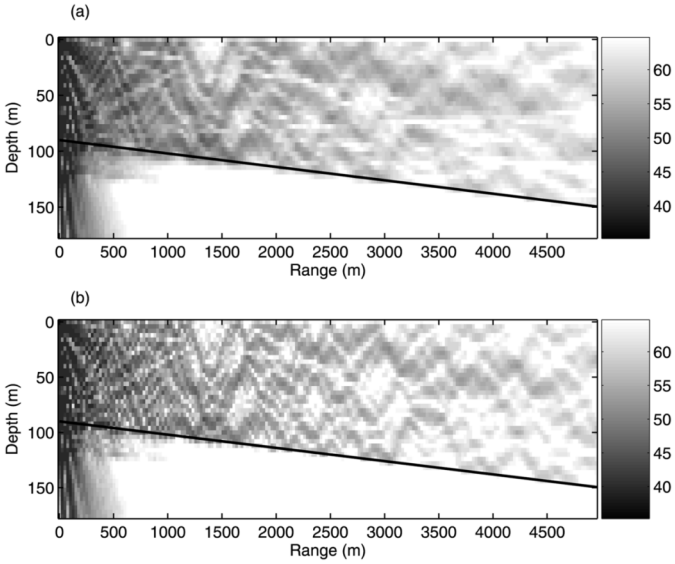

Fig. 6. Median TL (dB) based on (a) prior and (b) posterior distributions of environmental parameters.

out that the true bottom is considerably more complicated than the three-layered sediment model we are using. The inverted environmental parameters and their search bounds are indicated in Fig. 2(e).

Fig. 2 summarizes the whole inversion process (which is repeated from [23]). Detailed comments for each panel are provided as follows.

a) A contour plot of the TL (dB) derived from the most likely (best-fit) environmental model.
b) The comparison of observed TL (solid) and predicted TL (dashed) at 250 Hz for both the 20 and 85 m deep array (the TL at 85 m has been offset downward 25 dB). Note that data from this frequency has not been used in the inversion and is thus a test of how well the inversion performed on the vertical array data.
c) The match of the observed data (solid) and inverted field (dashed) on the vertical array at the frequencies (50 and 300 Hz) used in the inversion.
d) The obtained (dashed) and true (solid) bottom sound-speed profiles.
e) The posterior distributions for the inverted model parameters.

Having found a good environmental parametrization and a model parameter estimate, a second inversion run is carried out

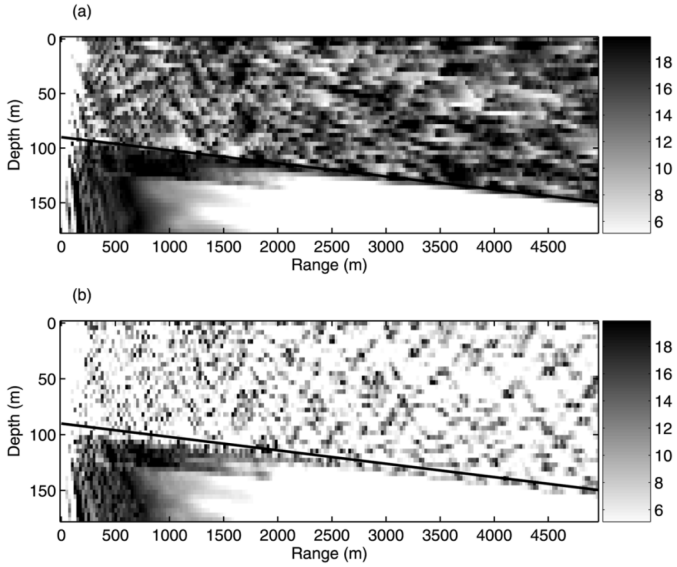

Fig. 7. Range (dB) between fifth and ninety fifth percentiles of the TL for (a) prior and (b) posterior probabilities.

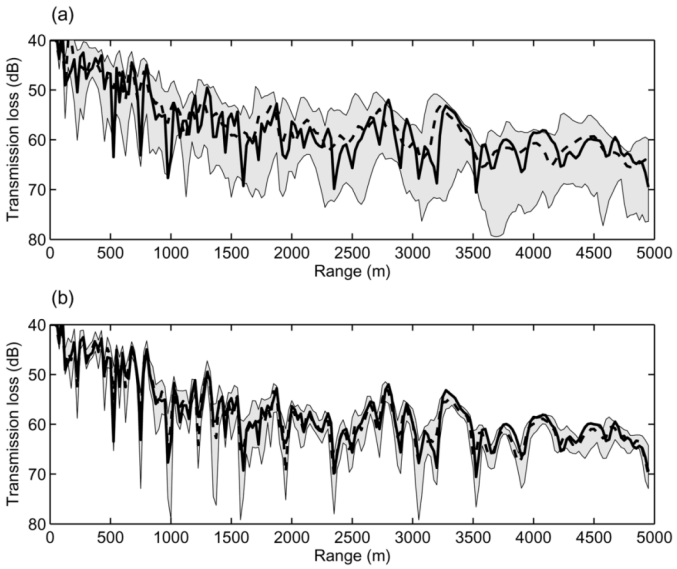

Fig. 8. Median TL (dashed) and the true TL (heavy solid) at 80-m depth based on all (a) prior samples and (b) posterior samples. The gray area indicates the range between the fifth and ninety fifth percentiles.

to estimate the posterior distribution of the bottom sound-speed profile, as shown in Fig. 3. All other parameters are kept at their optimal values found in the first inversion. We select arbitrarily a three layer model for the bottom profile, however, a more systematic approach would be to use evidence testing to find the most likely environmental parametrization [15]. We vary the following four parameters: The layer-1 sound speed, the increase in sound speed for layer-2 (from layer-1), the increase in sound speed for layer-3 (from layer-2), and the basement sound-speed increase (from layer-3). For each parameter the search interval is discretized by 20 values. The upper and lower bounds of the search interval are indicated in Fig. 3. The likelihood function is evaluated exhaustively over the entire grid of 160 000 (20^4) samples.

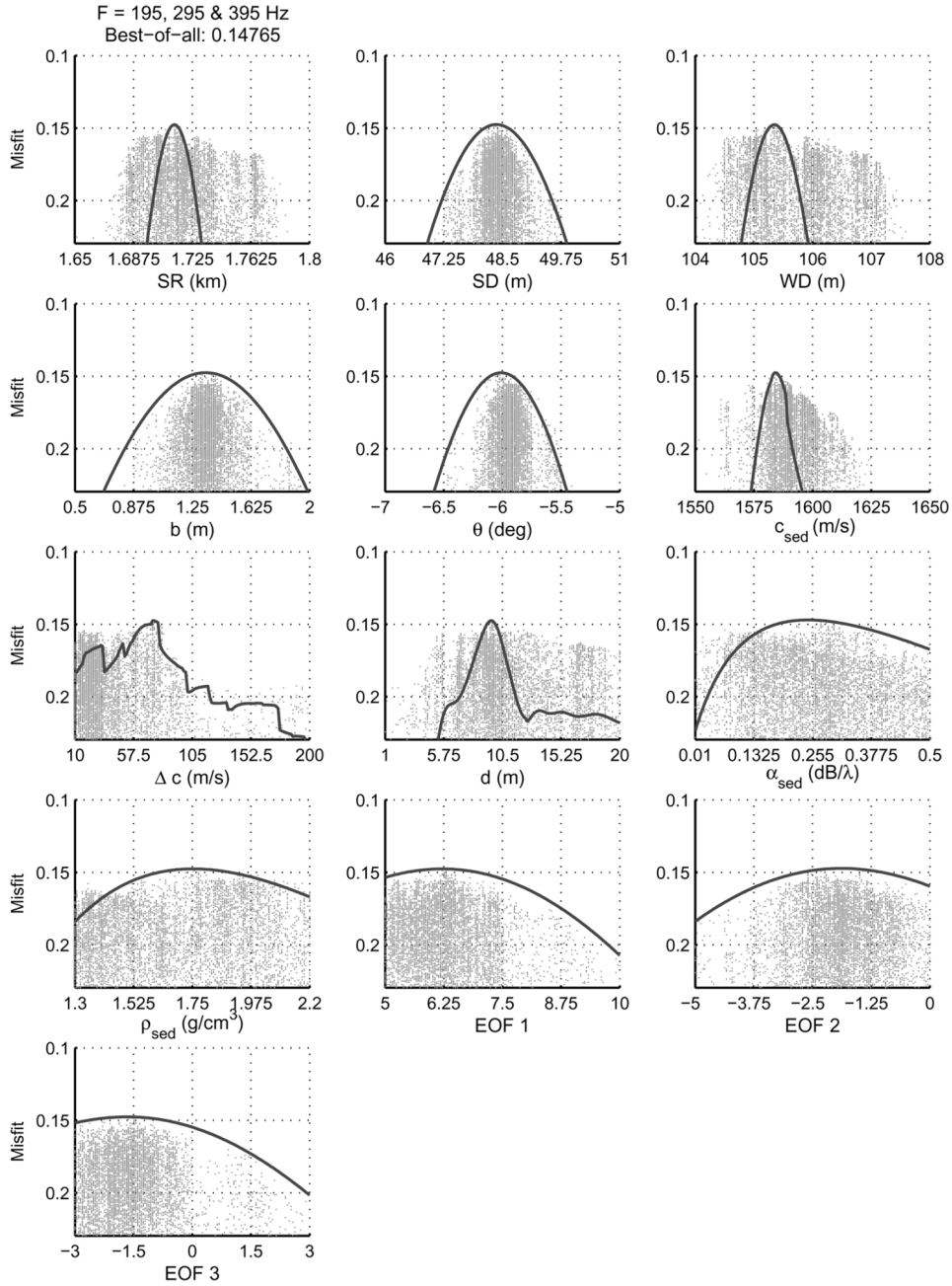

Fig. 9. Marginal scatter diagrams of the SAGA search for the model parameters. The vertical axis represents the attained misfit on a linear scale. The thick line is the sensitivity curve of the multifrequency objective function using the best-fit model as a baseline.

B. TC1—TL Prediction

All of the 160 000 samples are used for predicting the statistics of transmission loss at 250 Hz, 0–5 km in range, and 0–200 m in depth. For computing the prior field, each parameter is weighted uniformly with bounds as indicated in Fig. 3. While for the posterior field, each model parameter is weighted according to their posterior distribution in Fig. 3.

Using these 160 000 samples, the probability distribution for the TL is computed at 80-m depth as a function of range (Fig. 4). The prior distribution is wider and the nulls are less sharp than the nulls for the posterior distribution. This can easily be seen by making a line plot (Fig. 5) of the prior (dashed) and posterior (solid) probabilities of TL at a range of 4200 m.

The prior and posterior median TL-fields are computed, Fig. 6. There is less structure in the prior TL field than in the posterior field. This is because the main parameters are more constrained. The spread in the prior and posterior fields is defined as the range between the fifth and ninety fifth percentiles and is plotted in Fig. 7. It is seen that the spread in the water column for the posterior TL is much less than that for the prior TL. At shorter ranges (less than 1 km), the posterior field shows a large spread in the bottom. This may be a consequence of the choice of the bottom model, which is much more simple than the true bottom.

However, as seen in Fig. 7, this modeling error has limited influence on the predicted wave field in the far-field bottom or near-field water column. At shorter ranges, the sound field in

the water column has fewer interactions with the bottom, due to the higher attenuation for the higher angle rays (higher-order modes). At longer ranges, the resolving power of the surviving low-order modes is consistent with the simple bottom model.

A practical way to display the uncertainty is to plot the median TL (dashed) combined with the fifth and ninety fifth percentiles (represented by the gray area), as shown in Fig. 8. Clearly, the posterior spread is decreased significantly. Based on the true environment [19] the true TL (heavy solid) is computed. Because the environmental model used in the inversion is a simplification over the true model, it is not clear how the true TL curve should relate to the median or spread of the posterior TL distribution. However, most of the true TL (black) is within the spread (gray area) of the TL distribution.

It is interesting to notice that the range of the posterior probability (gray area) in Fig. 8 is larger than the prior at certain points in range. These points correspond to the ranges where the field is close to a null, causing large variations in the field.

C. Asiaex—Inversion

Data from the 2001 East China sea experiment (see [20]) also are used to illustrate the method. A 16-element vertical line array (VLA) was deployed in 105-m deep water. The source was towed at a depth of about 48.5 m. The seafloor model consists of an ocean layer overlying a sediment layer atop of a basement. All layers are assumed to be range independent. Matched-field geoacoustic inversion using the selected frequencies 195, 295, and 395 Hz was carried out at $T = 29$ min. Based upon the GPS position of R/V Melville, the source was approximately 1.7 km away from the VLA. An environmental domain of 13 parameters, as indicated in Fig. 9 (with their search bounds), including geometrical, geoacoustic, and ocean sound-speed empirical orthogonal functions (EOF) coefficients is inverted for.

Fig. 9 shows the marginal dot diagrams for the model parameters. The vertical axis is the achieved misfit using a Bartlett objective function with respect to the parameter sampled during the SAGA optimization [1]. For each parameter, a simple parameter sensitivity (solid curve) was computed by keeping the other parameters fixed at the optimal point and just varying the one parameter. We see that the sampled values for the array bow and tilt parameters (b and θ) are spread mainly inside the sensitivity curve and align mostly with the best-fit values. A similar behavior is observed for the ocean sound-speed EOF coefficients but with a wider span. The consistency between the local (solid curve) and global (dots) searches shows that this set of parameters is weakly correlated with the other parameters. For the geoacoustic parameters, most sampled values wander outside the parameter sensitivity (solid curve). This reveals the more complicated structure of the multidimensional search space. Note that the sampled values for the source range (sr) and the water depth (wd) are spread uniformly throughout the range of the parameter interval. This is due to the strong coupling between these two parameters as can be observed by computing the 2-D marginal distribution between these two parameters.

A second inversion is now carried out to determine the uncertainty for two of the most important model parameters. For simplicity, we assume that only water depth (wd) and sediment

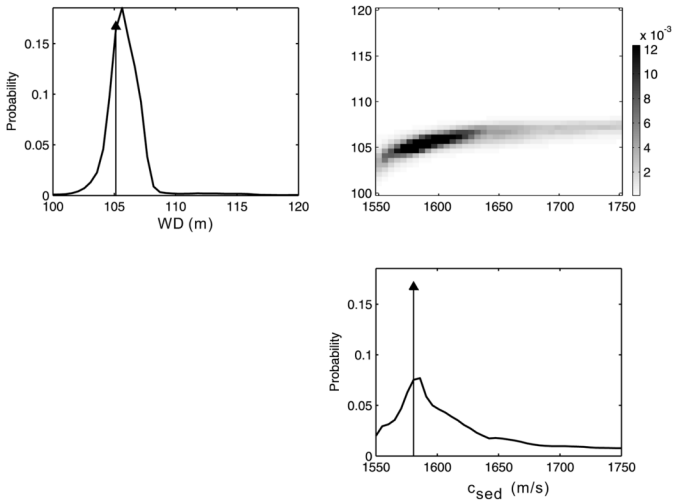

Fig. 10. Marginal probabilities for water depth (wd) and sediment sound speed ($c_{\rm sed}$). The contour plot shows the 2-D distribution. The vertical arrow indicates the ML solution (SAGA best-fit model). Note that the maximum in the marginal distribution might not correspond to the ML estimate.

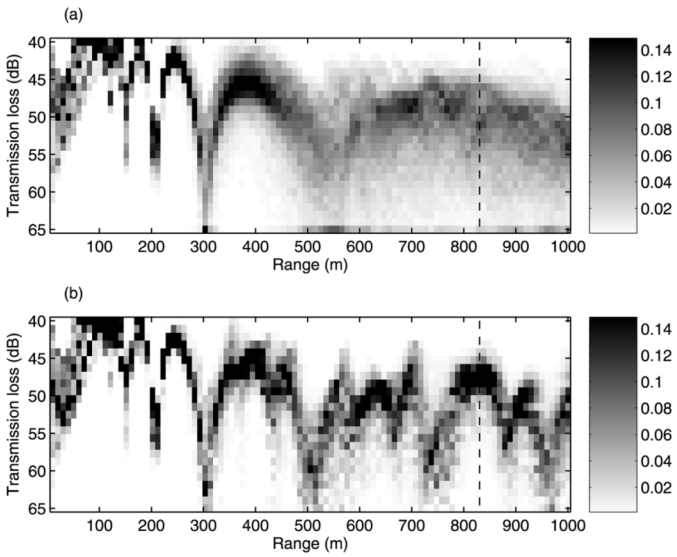

Fig. 11. (a) Prior and (b) posterior probability distributions for TL versus range at 50-m depth.

sound speed ($c_{\rm sed}$) have any associated uncertainty. All other parameters are fixed at the optimal values found in the inversion detailed above. Varying only the above two parameters gives posterior probability indicated in Fig. 10. It is based on the likelihood formulation (9) and using the same data as in the full inversion.

D. ASIAEX—TL Prediction

The posterior probability (Fig. 10) is used to compute the posterior probability $\mathbf{u}$ using a frequency of 500 Hz and a source depth of 20 m. Except for water depth (bounds 100–120 m) and bottom sound speed (bounds 1550–1750 m/s), we keep the environment fixed at the values found in the inversion. In the present application, we evaluate this using grid integration. First, the probability for TL at mid-water depth (50 m) is evaluated (Fig. 11). The prior probability assumes evenly weighting

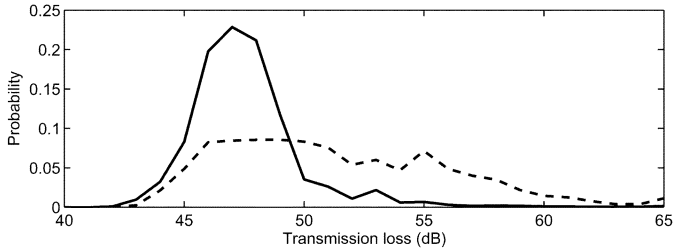

Fig. 12. Posterior (solid) and prior (dashed) probabilities of TL at 830-m range and 50-m depth. These correspond to a cut (vertical dashed lines) through the contours in Fig. 11.

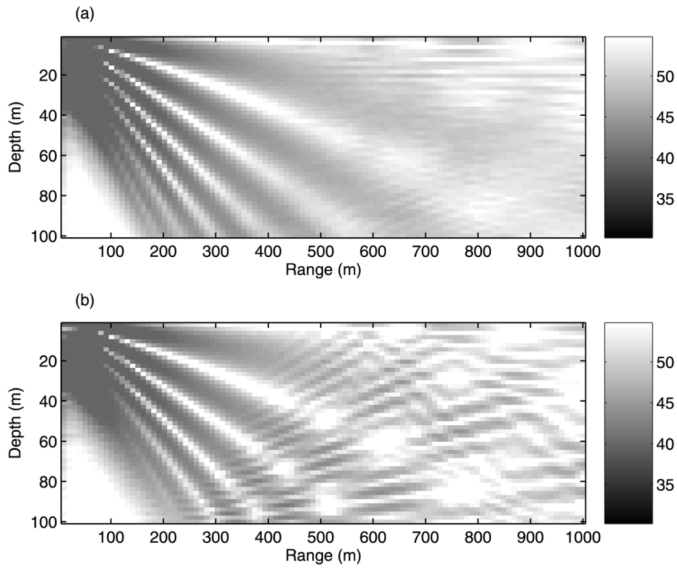

Fig. 13. Median TL (dB) based on (a) prior and (b) posterior distributions of the environmental parameters (water depth and sediment sound speed).

of all the explored environmental models with the same bounds as above. The prior distribution is a) spread out over a wide range but the posterior distribution and b) more narrow. For the first 200 m, the transmission loss is only little influenced by the waveguide parameters and thus there is little difference between posterior and prior distributions. We then examine the probability at one point (50-m depth and 830-m range). This is done by taking a cut through the contour plots in Fig. 11 at 830-m range (indicated by a vertical dashed line, corresponding to a peak in TL curve), as shown in Fig. 12. The posterior (solid) is much more concentrated than the prior (dashed).

Contours of the median TL then are computed for the prior and posterior fields (Fig. 13). A good way to understand the uncertainty is to plot the fifth to ninety fifth percentile ranges (gray area) of the prior and posterior fields, Fig. 14. Close to the source, there is little uncertainty for both prior and posterior fields as the sound field is not influenced by the waveguide parameters. Further away from the source, the prior uncertainty increases earlier in range than the posterior does, as the waveguide parameters are less well determined. It also is seen that around the nulls of the median fields (Fig. 13) the variations in the fields are the largest (Fig. 14).

The uncertainty is easily conveyed by plotting the median TL (heavy solid) combined with the fifth and ninety fifth percentiles (represented by the gray area), see Fig. 15. Similar to the results

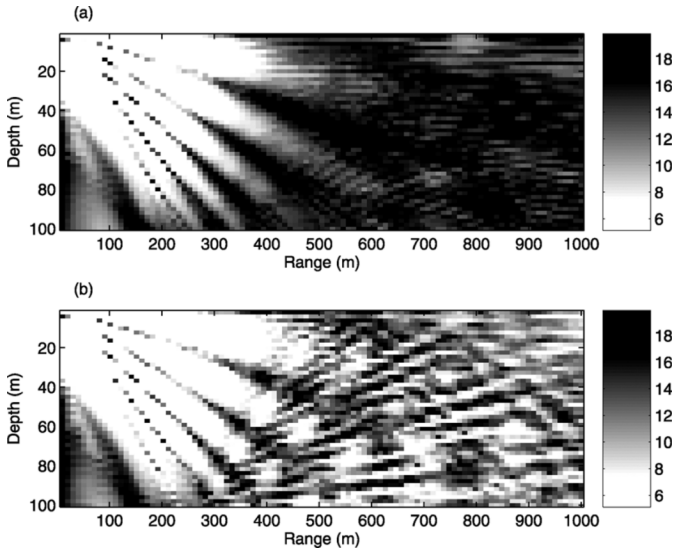

Fig. 14. Range (dB) between fifth and ninety fifth percentiles of the TL for (a) prior and (b) posterior probabilities.

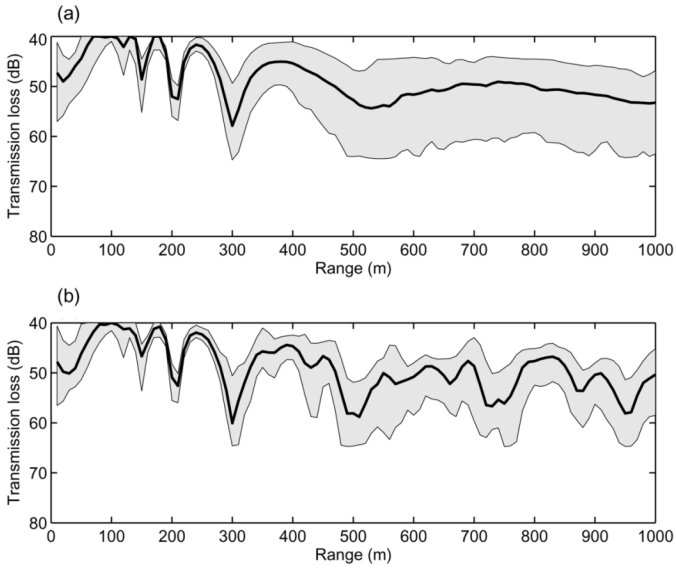

Fig. 15. Median TL (solid) at 50-m depth based on all (a) prior samples and (b) posterior samples. The gray area indicates the range between the fifth and ninety fifth percentiles.

for TC1, Section III-B, it is observed that the posterior probabilities have the largest spread around the nulls of the median field. Overall, the posterior spread has decreased significantly.

IV. Conclusion

An approach for predicting the statistical properties of transmission loss based on the result from a probabilistic-based geoacoustic inversion has been developed using a likelihood formulation. The likelihood function assumes the error in the observed data is Gaussian. The presented examples used acoustic data on vertical arrays for the inversion, however, any data could be used. The result of this inversion is a probabilistic-based description of the environmental parameters. The environmental parameters are mapped via their probability distributions into a probability distribution of transmission loss.

In the transmission loss domain, we can compute the full posterior distribution at all frequencies, ranges and depths. In the examples, we demonstrated how to use the full transmission loss probability distribution and extracted characteristic features such as median and lower/upper percentiles from this distribution.

ACKNOWLEDGMENT

The authors would like to thank P. Abbot for constructive comments on the manuscript.

REFERENCES

[1] P. Gerstoft, "Inversion of seismoacoustic data using genetic algorithms and *a posteriori* probability distributions," *J. Acoust. Soc. Amer.*, vol. 95, no. 2, pp. 770–782, Feb. 1994.

[2] P. Gerstoft and C. F. Mecklenbräuker, "Ocean acoustic inversion with estimation of *a posteriori* probability distributions," *J. Acoust. Soc. Amer.*, vol. 104, no. 2, pp. 808–819, Aug. 1998.

[3] M. I. Taroudakis and M. G. Markaki, "Bottom geoacoustic inversion by "broadband" matched field processing," *J. Comp. Acoust.*, vol. 16, no. 2, pp. 167–183, 1998.

[4] L. Jaschke and N. R. Chapman, "Matched field inversion of broadband data using the freeze bath method," *J. Acoust. Soc. Amer.*, vol. 106, no. 4, pp. 1838–1851, Oct. 1999.

[5] G. R. Potty, J. H. Miller, J. F. Lynch, and K. Smith, "Tomographic inversion for sediment parameters in shallow water," *J. Acoust. Soc. Amer.*, vol. 108, no. 3, pp. 973–986, Sep. 2000.

[6] S. E. Dosso, "Quantifying uncertainty in geoacoustic inversion I: A fast Gibbs sampler approach," *J. Acoust. Soc. Amer.*, vol. 111, no. 1, pp. 129–142, Jan. 2002.

[7] D. P. Knobles, R. A. Koch, L. A. Thompson, K. C. Focke, and P. E. Eisman, "Broadband sound propagation in shallow water and geoacoustic inversion," *J. Acoust. Soc. Amer.*, vol. 113, no. 1, pp. 205–222, Jan. 2003.

[8] F. B. Jensen and N. Pace, *Impact of Littoral Environmental Variability on Acoustic Predictions and Sonar Performance*, The Netherlands: Kluwer, 2002.

[9] P. Abbot and I. Dyer, "Sonar performance predictions based on environmental variability," in *Impact of Littoral Environmental Variability on Acoustic Predictions and Sonar Performance*, N. G. Pace and F. B. Jensen, Eds., The Netherlands, 2002, pp. 611–618.

[10] K. Mosegaard and A. Tarantola, "Probabilistic approach to inverse problems," in *International Handbook of Earthquake & Engineering Seismology, Part A*: Academic Press, 2002, pp. 237–265.

[11] L. T. Rogers, M. Jablecki, and P. Gerstoft, "Posterior distribution of a statistic of propagation loss estimated from radar sea clutter," *Radar Science*, vol. 40, no. 6, 2005. RS6006.

[12] A. Tarantola, *Inverse Problem Theory and Methods for Model Parameter Estimation*. Philadelphia, PA: SIAM, 2005.

[13] M. K. Sen and P. L. Stoffa, "Bayesian inference, Gibbs' sampler and uncertainty estimation in geophysical inversion," *Geophys. Prosp.*, vol. 44, no. 2, pp. 313–350, Feb. 1996.

[14] K. Mosegaard and M. Sambridge, "Monte Carlo analysis of inverse problems," *Inverse Problems*, vol. 18, no. 3, pp. 29–54, Jul. 2002.

[15] D. Battle, P. Gerstoft, W. S. Hodgkiss, W. A. Kuperman, and P. Nielsen, "Bayesian model selection applied to self-noise geoacoustic inversion," *J. Acoust. Soc. Amer.*, vol. 116, no. 4, pp. 2043–2056, Oct. 2004.

[16] D. J. C. MacKay, *Information Theory, Inference and Learning Algorithms*. Cambridge, U.K.: Cambridge Univ. Press, 2003.

[17] C. F. Mecklenbräuker and P. Gerstoft, "Objective functions for ocean acoustic inversion derived by likelihood methods," *J. Comp. Acoust.*, vol. 8, no. 2, pp. 259–270, Feb. 2000.

[18] F. B. Jensen and M. C. Ferla, "SNAP: The SACLANTCEN Normal-Mode Acoustic Propagation Model," SACLANT Undersea Research Centre, La Spezia, Italy, Tech. Rep., 1979.

[19] N. R. Chapman, A. S. Chi-Bing, D. King, and R. B. Evans, "Benchmarking geoacoustic inversion methods in range dependent waveguides," *IEEE J. Ocean. Eng.*, vol. 28, no. 3, pp. 320–330, Jul. 2003.

[20] C.-F. Huang and W. S. Hodgkiss, "Matched field geoacoustic inversion of low frequency source tow data from the ASIAEX East China Sea experiment," *IEEE J. Ocean. Eng.*, vol. 29, no. 4, pp. 952–963, Oct. 2004.

[21] P. Gerstoft, "SAGA users guide 5.0, an inversion software package," in *SAGA Users Guide 2.0, an Inversion Software Package*. La Spezia, Italy: SACLANT Undersea Research Centre, 1997.

[22] M. D. Collins, "A split-step padé solution for the parabolic equation method," *J. Acoust. Soc. Amer.*, vol. 93, no. Apr., pp. 1736–1742, 1993.

[23] P. Gerstoft, W. S. Hodgkiss, W. A. Kuperman, and H. Song, "Phenomenological and global optimization inversion," *IEEE J. Ocean. Eng.*, vol. 28, no. 3, pp. 342–354, Jul. 2003.

Peter Gerstoft received the M.Sc. and the Ph.D. degrees from the Technical University of Denmark, Lyngby, Denmark, in 1983 and 1986, respectively, and the M.Sc. degree from the University of Western Ontario, London, ON, Canada, in 1984, all in civil engineering.

From 1987 to 1992, he was with Ødegaard and Danneskiold-Samsøe, Copenhagen, Denmark, working on forward modeling and inversion for seismic exploration. During that time, he spent one year as a Visiting Scientist at the Massachusetts Institute of Technology, Cambridge. From 1992 to 1997, he was a Senior Scientist at SACLANT Undersea Research Centre, La Spezia, Italy, where he developed the SAGA inversion code, which is used for ocean acoustic and electromagnetic signals. Since 1997 he has been with Marine Physical Laboratory, University of California, San Diego. His research interests include global optimization, modeling and inversion of acoustic, and elastic and electromagnetic signals.

Dr. Gerstoft is a Fellow of Acoustical Society of America and elected member of the International Union of Radio Science, Commission F.

Chen-Fen Huang (S'01) received the B.S. and M.S. degrees in marine environment, in 1995 and 1997, respectively, and the M.S. degree in undersea technology in 1998, all from National Sun Yat-sen University, Kaohsiung, Taiwan. She received the Ph.D. degree in oceanography specializing in geoacoustic inversion from the Scripps Institution of Oceanography, University of California, San Diego, in 2005.

From 1998 to 2000, she worked as a Research Assistant at the Institute of Undersea Technology, National Sun Yat-sen University. Currently, she is a Postdoctoral Researcher at the Scripps Institution of Oceanography. Her research interests include underwater geoacoustic exploration, sediment acoustics, underwater signal processing, and acoustic wave scattering from rough surfaces.

Dr. Huang is a member of the Acoustical Society of America.

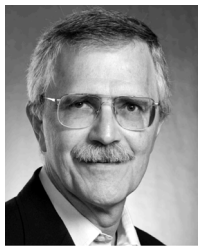

William S. Hodgkiss (S'68–M'75) was born in Bellefonte, PA, on August 20, 1950. He received the B.S.E.E. degree from Bucknell University, Lewisburg, PA, in 1972, and the M.S. and Ph.D. degrees in electrical engineering from Duke University, Durham, NC, in 1973 and 1975, respectively.

From 1975 to 1977, he worked at the Naval Ocean Systems Center, San Diego, CA. From 1977 to 1978, he was a faculty member in the Electrical Engineering Department, Bucknell University, Lewisburg, PA. Since 1978, he has been a member of the faculty of the Scripps Institution of Oceanography, University of California, San Diego, and on the staff of the Marine Physical Laboratory, University of California, San Diego, where currently he is a Deputy Director. His present research interests are in the areas of adaptive array processing, propagation modeling, and environmental inversions with applications of those to underwater acoustics and electromagnetic wave propagation.

Dr. Hodgkiss is a Fellow of the Acoustical Society of America.